Research Article

Ethanol extract of *Poria cocos* induces apoptosis and differentiation in Neuro-2a neuroblastoma cells

Ethanol extract of *Poria cocos* induces apoptosis and differentiation in Neuro-2a neuroblastoma cells

Xia Jiang, Jie Xie, Zhaotun Hu, and Xiaoliang Xiang

Key Laboratory of Research and Utilization of Ethnomedicinal Plant Resources of Hunan Province，College of Biological and Food Engineering, Huaihua University, Huaihua, China.

Abstract

Poria cocos is a widely used ingredient in traditional Chinese medicine and dietary supplement. In this study, the effects of the ethanol extract of *P. cocos* on cell proliferation in Neuro-2a neuroblastoma cells and its possible mechanism of action are investigated. The extract inhibited the growth of Neuro-2a cells in a dose-dependent manner with an IC_{50} value of 34.6 μg/mL. To further elucidate the mechanism by which the extract acts, transcriptome analysis using high-throughput Illumina RNA-seq technology was performed. Transcriptome analysis revealed that the cell cycle as the potential primary target pathway of the extract in Neuro-2a cells. Flow cytometry analysis confirmed that the extract induced cell cycle arrest at G1 phase. Furthermore, the extract also induced apoptosis in Neuro-2a cells. Notably, it was found that Neuro-2a cells exhibited morphological features of differentiation when treated with the extract. This study suggests that *P. cocos* may be a potential candidate therapeutic agent in combating neuroblastoma.

Introduction

Neuroblastoma arises from the sympathetic nervous system and is the most common solid tumor in children throughout the world. It is the second most frequent malignancy in infancy after lymphoblastic leukemia (Maris et al., 2007). Meanwhile, it is one of the most challenging malignant tumors because of its heterogeneity, diversity of clinical behavior, and high recurrence (Brodeur, 2003).

Most of the cases are treated with conventional therapeutic approaches, including surgery, external beam radiation therapy and cytotoxic chemotherapy. Chemotherapeutic drugs include cyclophosphamide, doxorubicin and cisplatin (Berthold et al., 2000). Immunotherapy includes the use of regorafenib, dinutuxi-mab, naxitamab, etc (Dong et al., 2019).

However, high-risk neuroblastoma is still one of the most difficult tumors to cure, the overall 5-year survival rate for patients is less than 40% (Brodeur, 2003). Therefore, there is an urgent need for novel chemotherapeutic agents for the treatment of neuroblastoma.

Natural products include thousands of compounds that exist in fruits, vegetables, plants, and herbs, and several clinical anti-cancer drugs have been derived from natural products (Gordaliza et al., 2007).

Various natural products are also reported to have inhibitory activities against neuroblastoma. For instance, sparstolonin B derived from *Sparganium stoloniferum* inhibits the growth of neuroblastoma cells by arresting the cell cycle at G2/M phase (Kumar et al., 2014). Cucurbitacin B isolated from *Trichosanthes kirilowii*, inhibits neuroblastoma cell proliferation through up-regulation of PTEN (Shang et al., 2014). To date, numerous natural products such as withaferin A, honokiol, vincristine, apigenin, quercetin, and β-carotene proved to possess

anti-tumor activities on neuroblastoma cells (Mallepalli et al., 2019). Thus, the development of compounds with anti-neuroblastoma effects from natural products has currently become a very important topic.

Poria cocos (Schw.) Wolf with the homology of medicine and food is a famous traditional Chinese medicine (Pfy et al., 2019). The dried sclerotia of *P. cocos* has frequently been used as a tonic to benefit the internal organs and is prescribed as one of the chief ingredients in compound prescriptions in traditional oriental medicine. More particularly, this fungus is widely used in traditional medicine to treat chronic gastritis, acute gastroenteric catarrh, gastric atony, edema, nephrosis, dizziness, nausea, and emesis (Lee et al., 2009; Tang et al., 2014). Previous studies have indicated that its extracts and components have a variety of biological activities such as antifungal and antibacterial, antioxidant, neuroprotective, anti-inflammatory, antiangiogenic, and anti-cancer effects (Canavate, 2010; Zhang et al., 2006; Cheng et al., 2013; Chang et al., 1991).

However, the effect of this drug on neuroblastoma has not been reported before. In the present study, the anti-cancer properties of the ethanol extract of *P. cocos* and the responsible underlying molecular mechanisms involved in neuroblastoma mouse model Neuro-2a cells were investigated.

Materials and Methods

Reagents

Poria cocos was purchased from Hunan Province, China.

Hoechst33342, primary antibodies against caspase 3, cleaved caspase 3, PARP, cleaved PARP, survivin, β-actin, HRP-conjugated anti-mouse and anti-rabbit were purchased from Beyotime Biotechnology (China). DMSO and MTT were purchased from Sigma (USA). Minimum Essential Medium Eagle, fetal bovine serum, penicillin, and streptomycin were obtained from Hyclone (USA). All other chemicals and reagents are of analytical grade.

Preparation of P. cocos extract

The ethanol extract of *P. cocos* was prepared according to Jeong et al (2014). The dried sclerotium of *P. cocos* was grounded into powder and extracted twice with 10 volumes of 80% ethanol at 85-90°C in a reflux condenser for 3 hours. After being filtered through a 0.2-μm filter, the extract was concentrated and lyophilized by vacuum evaporation. The solid form of the extract was dissolved in DMSO before the experiment.

Cell culture

Mouse neuroblastoma Neuro-2a cells were grown in Minimum Essential Medium Eagle supplemented with 10% heat-inactivated fetal bovine serum and 1% penicillin/streptomycin, and maintained at 37°C in 5% CO_2 humidified atmosphere. Cells were passaged every 3-4 days.

Cytotoxicity test

Cell viability was assessed by MTT (3,4,5-dimethyl-thiazol-2-yl)-2-5-diphenyltetrazolium bromide) reduction assay. For the assay, cells (5×10^3) were plated in 96-well microtiter plates and grown for 24 hours. After-

---

Box 1: Western Blotting

Principle

Western blotting is used to detect and characterize target proteins. The principle is based on immunochromatography where proteins are separated into polyacrylamide gel according to their molecular weight.

Requirements

BCA protein assay kit; Electrochemiluminescence detector; HRP-conjugated secondary antibody; Neuro-2a cells; Ethanol extract of *P. cocos*; Phosphate buffer solution; Polyvinylidene fluoride membrane; Primary antibody; RIPA buffer; Sodium dodecyl sulfate polyacrylamide gel

Procedure

Step 1: Neuro-2a cells were seeded in 35 mm dish (6×10^4/dish) overnight and then incubated with different concentration of *P. cocos* (10-50 μg/mL) for 24 hours at 37°C

Step 2: Remove the culture medium and wash the cells with ice-cold phosphate buffer solution. Cells were lysed in RIPA buffer containing protease and phosphatase inhibitors, incubate on ice for 10 min. Centrifuge at 12,000 rpm at 4°C for 15 min and collect supernatant for use

Step 3: Whole cell lysates were quantified using a BCA protein

assay kit according to the manufacturer's instructions

Step 4: Equal amounts of protein (20-30 μg) were subsequently separated by SDS-PAGE, and transferred to polyvinylidene fluoride (PVDF) membranes

Step 5: Block the membrane for 1 hour at room temperature using blocking buffer (1 × TBST containing 5% non-fat dry milk)

Step 6: Wash membrane three times with 1 × TBST for 5 min each. Incubate the membranes with primary antibody overnight at 4°C

Step 7: Wash membrane three times with 1 × TBST for 5 min each, then incubate the membrane with a suitable HRP-conjugated secondary antibody

Step 8: Wash membrane three times with 1 × TBST for 5 min each. Prepare ECL substrate according to the manufacturer's instructions

Step 9: Expose the membrane to autoradiography film in a darkroom

References

Jiang et., 2020; Xiang et al., 2016; Towbin et al., 1979

References (video)

Eslami and Lujan, 2010; Shen et al., 2021; Lim et al., 2021

ward, cells were treated with different concentrations of the ethanol extract (5, 10, 20, 50, and 100 µg/mL). After 24 hours of incubation, the media containing the extract were carefully removed and 100 µL of MTT solution (0.5 mg/mL in Minimum Essential Medium Eagle) was added to each well and further incubated for 4 hours. DMSO (200 µL) was added to each well to dissolve the formazon crystals, and the absorbance was measured by a micro-plate reader at 570 nm. Cell viability was shown relative to the control in a graph (Jiang et., 2020).

Apoptosis assay by Hoechst33342 and TUNEL staining

Hoechst33342 staining was used to detect apoptosis nuclear morphological changes after *P. cocos* treatment. Briefly, Neuro-2a cells were treated with *P. cocos* for 24 hours. Then cells were collected, washed, and stained with Hoechst33342 for 15 min before visualizing by fluorescence microscopy (Olympus, Japan). The TUNEL apoptosis detection kit (Abbkine, China) was used to detect apoptosis. The TUNEL assay was performed according to the manufacture's protocol (Eun-Seok et al., 2016).

Differential expression analysis by RNA-seq

Cells were cultured in 6 cm dishes with a seeding density of 1×10^6 cells per dish and incubated 24 hours. Cells were harvested after treatment with 50 µg *P. cocos* or with DMSO for 12 hours and each treatment had three duplicates. Total RNA was extracted using TRIzol reagent (Life Technologies, USA). Transcriptome sequencing was performed by Novogene Biotechnology Co., Ltd. (China) based on the Illumina Hiseq platform. Gene expression levels were determined by cufflinks in the form of fragments per kilobase of exon per million fragments mapped (FPKM). For differentially expressed gene analysis, we calculated log2 fold change value ($\log_2$FC) for each gene in treatment and control samples. Functional enrichment analysis including Gene Ontology and KEGG pathways was performed for the identified differentially expressed genes (Yang et al., 2021).

Cell cycle assay by flow cytometry

Cells were trypsinized and centrifuged at $350 \times g$ at 4℃ for 5 min, washed twice with ice-cold phosphate-buffered saline, and stained with propidium iodide buffer (4 µg/mL propidium iodide, 1% triton X-100, 0.5 mg/mL RNase A in phosphate-buffered saline). Stained cells were analyzed with a flow cytometer (Beckman Coulter Inc., USA) (Dickey et al., 2011).

Colony formation assays

For colony formation assays, Neuro-2a cells were seeded in a 6-well plate at a density of 3×10^3 per well and cultured for 7 days. The dishes were photographed, and the total colony numbers and types of colonies on the plates were evaluated under a microscope. Colonies with >50 cells were scored. Colony formation efficiency was determined by counting the combination-treated group colonies stained with crystal violet solution (Dickey et al., 2011).

Differentiation assay

For neurite outgrowth assay, Neuro-2a cells were seeded into 24-well plates at a density of 1×10^4 cells/mL and grown for 24 hours. After 24 hours of incubation, the culture medium was replaced with differentiation medium (Minimum Essential Medium Eagle supplied with 0.5% fetal bovine serum and 1% penicillin/streptomycin) containing different test compounds for 24 hours. Neuro-2a cells were captured and counted under a phase contrast microscope. Neurites were defined as a protrusion with lengths longer than one diameter of the cell body. The neurite length of each cell was measured by Image J software (Jiang et., 2020).

Statistical analysis

The results are expressed as the mean ± standard error of the mean. Data were subjected to Student's *t*-test or one-way analysis of variance (ANOVA) followed by Tukey's test to assess the differences between the relevant control and each experimental group. A value of $p < 0.05$ was considered statistically significant.

Results

Effect on the proliferation of Neuro-2a cells

Figure 1A shows a schematic of the sequential extraction process of *P. cocos*. Initially, the effect of the extract on the cell viability of Neuro-2a cells was tested. As shown in Figure B, the extract significantly reduced cell viability in a dose-dependent manner, with IC_{50} values of 34.6 µg/mL after 24 hours of treatment. Colony formation assay further confirmed that the extract inhibited the Neuro-2a cells proliferation in a dose-dependent manner (Figure 1C, D). These results suggested that *P. cocos* inhibited the proliferation of Neuro-2a cells *in vitro*.

Effect on the transcriptional level of Neuro-2a cells

To further explore the underlying mechanism of cell growth inhibition of *P. cocos* towards Neuro-2a cells, the cells were treated with 50 µg/mL *P. cocos* for 12 hours and used to perform a transcriptome analysis using high-throughput sequencing platform of Illumina Hiseq2500. Overall, we identified 390 genes as differentially expressed genes (DEGs) after being treated with *P. cocos*. Among them, 171 genes were up-regulated, while 219 genes were down-regulated after *P. cocos* treatment (Figure 2A). To understand the functions of the DEGs, all the DEGs were subjected to Gene Ontology (GO) enrichment analysis (Figure 2B). Interestingly, we found that most DEGs involved in the cell cycle-related pathway such as cell cycle, mitotic sister chromatid segregation, mitotic cell cycle process, sister

chromatid segregation, mitotic nuclear division, mitotic cell cycle, cell cycle process, cell division, and nuclear division. To further characterize the potential functional pathways altered by *P. cocos*, KEGG pathway enrichment analysis was performed (Figure 2C). Figure 2C displays the top 20 significantly enriched KEGG pathways for the DEGs. It is also interesting to note that most DEGs are related to the cell cycle pathway. These results indicate that the cell process of Neuro-2a cells was the most impacted function by *P. cocos*.

Effect on G1 phase cell cycle arrest and apoptotic cell death in Neuro-2a cells

To further confirm the RNA-seq results, the effect of *P. cocos* on the cell cycle was investigated by flow cytometric analysis (Figure 3A). When cells were treated with 50 µg/mL *P. cocos* for 24 hours, the percentage of cells at G1 phase increased slightly, accompanying a

decrease in S phase (from 35.9% to 25.4%) when compared with the untreated control cells. This result suggests that the growth inhibitory effect of *P. cocos* was the result of the block of the cell cycle at G1 phase. It was further evaluated whether the *P. cocos* growth inhibition could be due to effects on Neuro-2a cell cycle progression and inducing cell apoptosis. The apoptotic cells were detected by Hochest33342 staining (Figure 3B). The shrinkage of the nuclear membrane and chromatin condensation were observed in *P. cocos*-treated Neuro-2a cells, indicating the occurrence of apoptosis. Similarly, the TUNEL assay showed an increase in apoptotic cells, as evidenced by enhanced fluorescence, confirming that *P. cocos* induced apoptosis in Neuro-2a cells (Figure 3C). Furthermore, the expression profiles of proteins involved in apoptosis were examined (Figure 3D). Western blot analysis showed that *P. cocos* reduced the level of precursor caspase 3 and increased
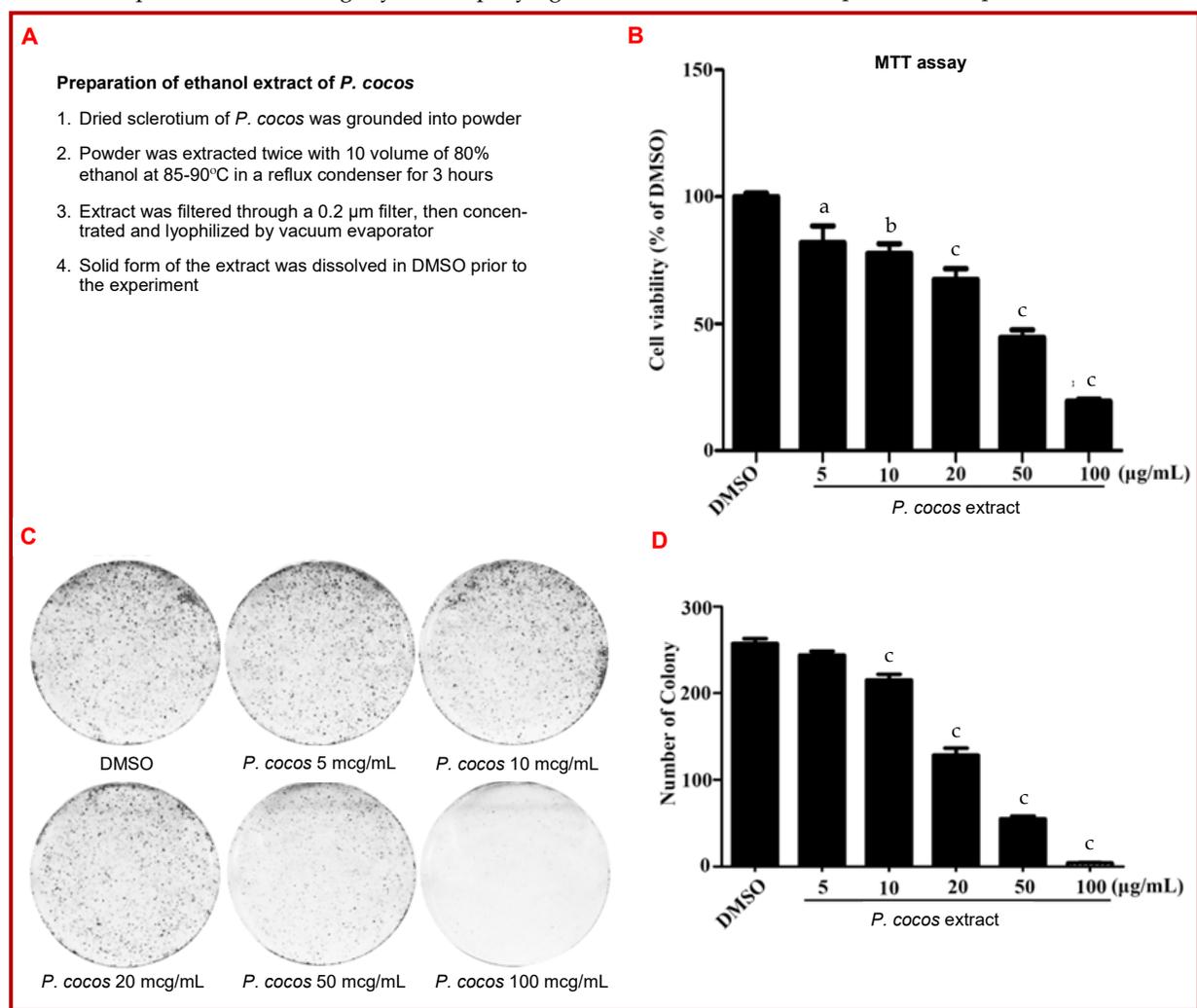

Figure 1: *P. cocos* inhibits the cell proliferation of Neuro-2a cells. Preparation of *P. cocos* ethanol extract (A). The percentages of viable cells treated with various concentration of *P. cocos* (5-100 µg/mL) for 24 hours, as measured by MTT assay (B). Colony formation of Neuro-2a cells treated with various concentrations of *P. cocos* (5-100 µg/mL), with staining by crystal violet (C, D). The results represent the mean ± SEM. (n=5). [a]p<0.05, [b]p<0.01, [c]p<0.001, indicated compound vs DMSO, one-way analysis of variance (ANOVA) followed by Dunnett's test
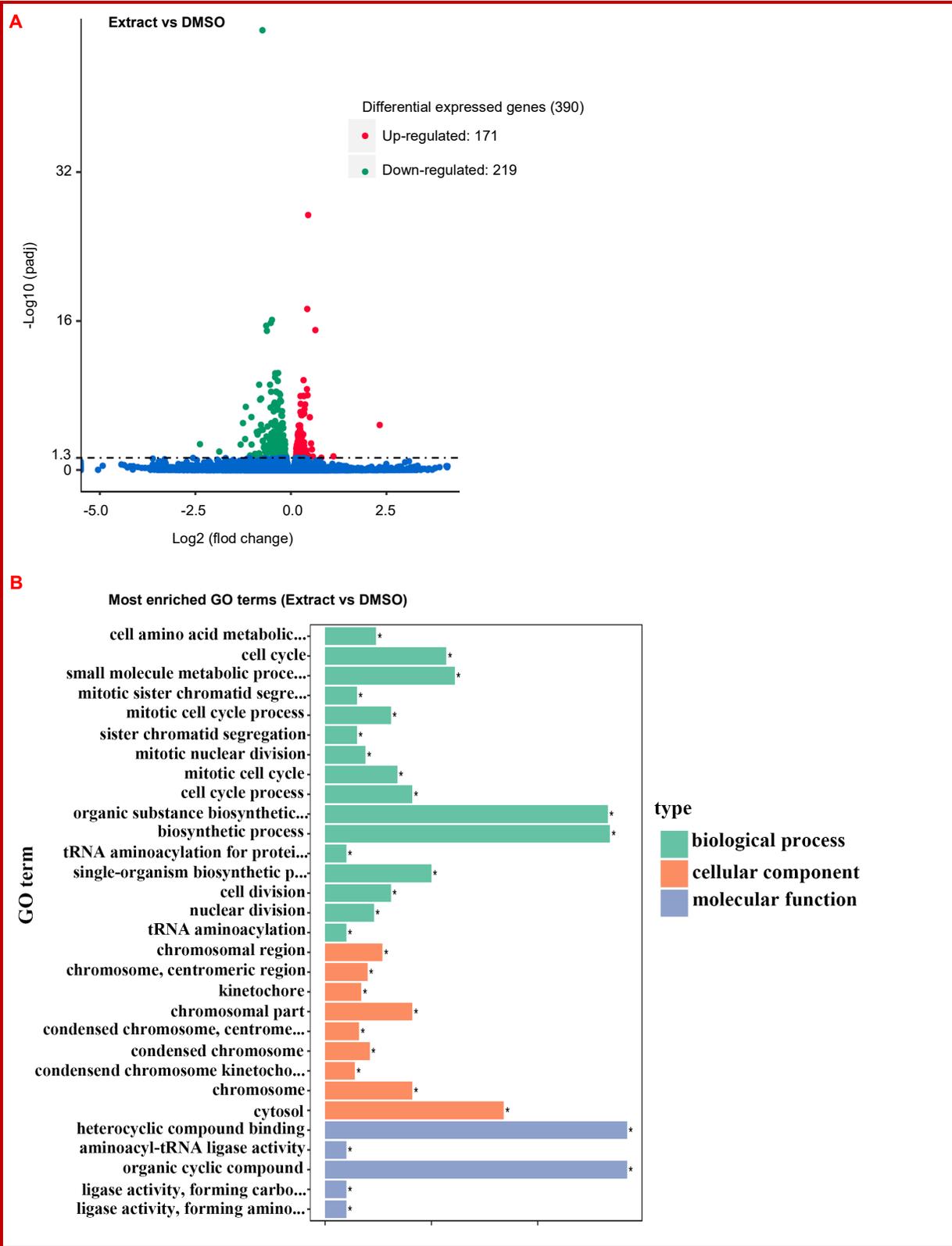
Figure 2: Differential gene expression analysis after treated with *P. cocos*. Volcano plots of differentially expressed genes between treated lycorine with control (A). GO enrichment analysis of regulated differentially expressed genes in *P. cocos*-treated cells. Histograms of the top 30 enriched GO terms. Enriched items were selected with a corrected. *p*-Value 0.05 (B). KEGG pathway enrichment analysis of regulated differentially expressed genes in *P. cocos* treated-cells (C). Scatter plots of the top 20 enriched KEGG pathway terms. Enriched items were measured by the rich factor, *q* value (q < 0.05) and the number of genes

C

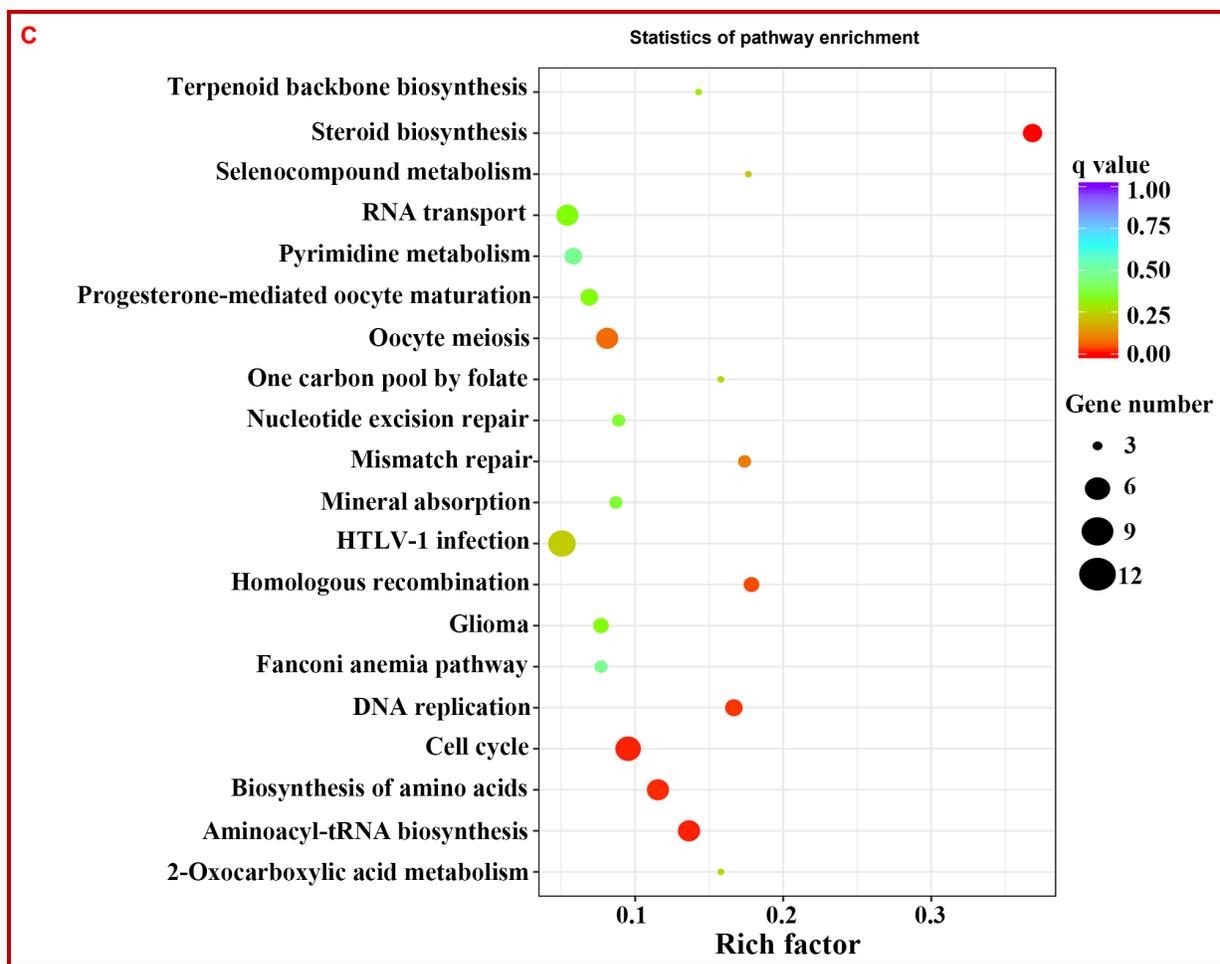**Statistics of pathway enrichment**

Figure 2: Differential gene expression analysis after treated with *P. cocos*. Volcano plots of differentially expressed genes between treated lycorine with control (A). GO enrichment analysis of regulated differentially expressed genes in *P. cocos*-treated cells. Histograms of the top 30 enriched GO terms. Enriched items were selected with a corrected. *p*-Value 0.05 (B). KEGG pathway enrichment analysis of regulated differentially expressed genes in *P. cocos* treated-cells (C). Scatter plots of the top 20 enriched KEGG pathway terms. Enriched items were measured by the rich factor, *q* value (q<0.05) and the number of genes (Cont…)

the level of cleaved caspase 3. Moreover, the caspase 3 downstream substrate PARP (cleaved PARP) accumulation. On the contrary, the anti-apoptotic protein survivin expression was significantly down-regulated after the treatment. These results demonstrated that *P. cocos* had an inhibitory effect on Neuro-2a cell cycle progression, which may trigger apoptosis in Neuro-2a cells.

Differentiation in Neuro-2a cells

Cell cycle regulation plays an important role in cell proliferation, apoptosis, and differentiation. We further evaluated the impact of *P. cocos* on Neuro-2a cell differentiation. Neuro-2a cells were treated with *P. cocos* at various concentrations (5-20 µg/mL) for 48 hours and retinoic acid (RA, 10 µM) was used as a positive control. The morphological changes were captured with a phase contrast microscope (Figure 4A). The results show that the untreated cells (DMSO) having a round shape with few neurites and the RA-treated cells developed exten-

sive neurite extensions. Notably, all aspects we examined, including differentiation rate (Figure 4B) and the longest neurite length (Figure 4C), *P. cocos* exhibited stronger activities. Moreover, *P. cocos* promoted Neuro-2a cell differentiation in a concentration-dependent manner.

Discussion

This study shows that *P. cocos* inhibits the proliferation and colony formation of Neuro-2a cells. Furthermore, it was tried to find out the mechanisms of anti-cancer activity of *P. cocos*.

RNA-seq-based-comparative transcriptome analysis has been extensively used to investigate the molecular mechanisms of drug action. Here, RNA-seq technology was used to detect the changes in gene expression in Neruo-2a cells after *P. cocos* treatment, to explain the molecular mechanism of its anti-tumor activity. After
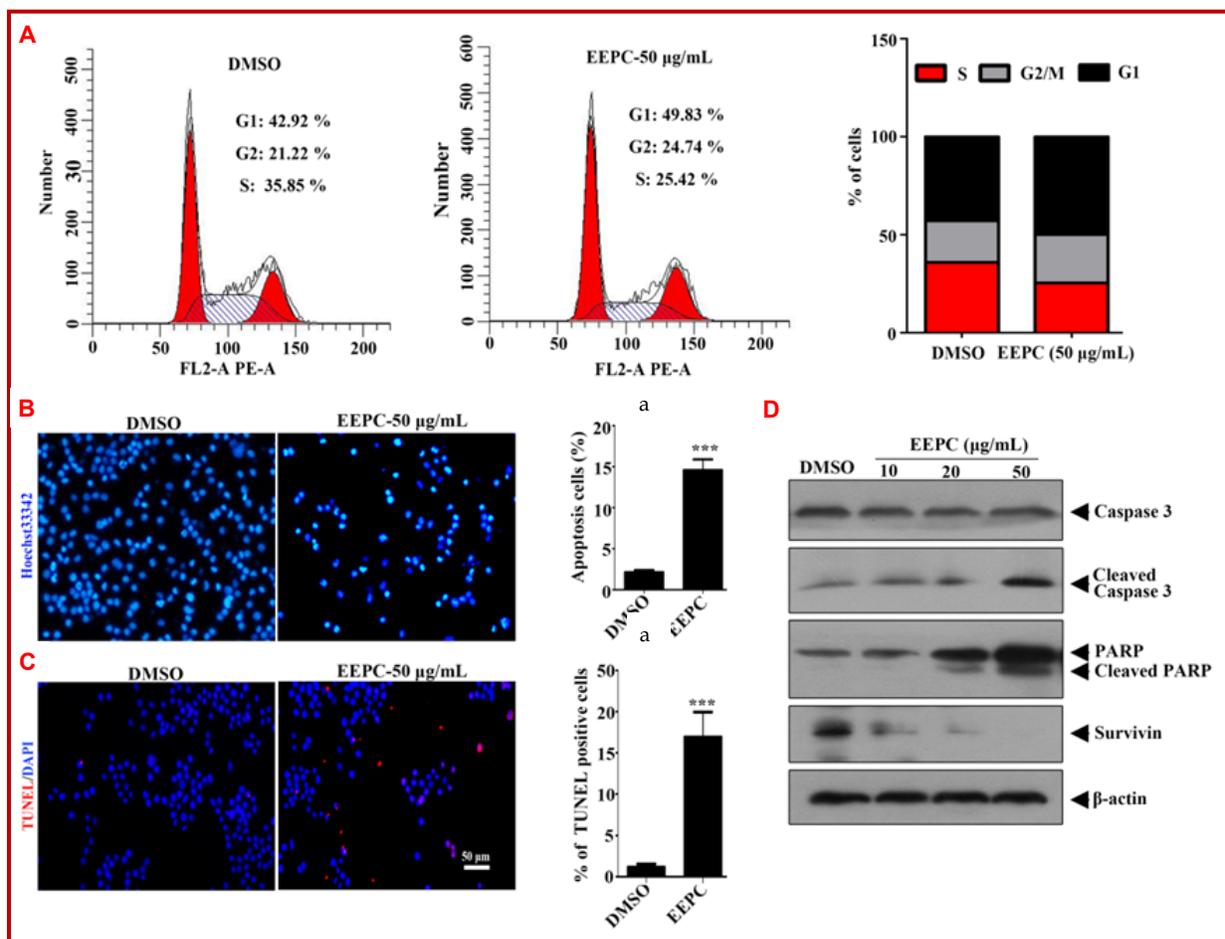
Figure 3: Effect of *P. cocos* (EEPC) on Neuro-2a cell cycle and apoptosis. The cell cycle was assayed by flow cytometry. The percentages of cell cycle phases were displayed in bar charts (A). Apoptosis cells were detected using Hoechst33342 fluorescent staining. Neuro-2a cells were treated with *P. cocos* (50 µg/mL) for 24 hours.) (B). Cell apoptosis were determined by the TUNEL assay. TUNEL-positive cells are labeled were red fluorescent. Nuclei were stained with DAPI (blue), Scale bar, 50 µm. Bar graph showed the percentage of apoptotic cells. Error bars represent SEM (n = 3). [a]$p<0.001$, indicated compound vs DMSO, one-way analysis of variance (ANOVA) followed by Tukey's test (C). Neuro-2a cells were treated with various concentration of *P. cocos* (10, 20 and 50 µg/mL) for 24 hours. The expression of caspase 3, cleaved-caspase 3, PARP, cleaved-PARP and survivin were analyzed by Western blot analysis (D)

treatment of *P. cocos*, 390 DEGs were detected, with 171 up-regulated and 219 down-regulated. Functional annotation including GO and KEGG analysis highlighted that most DEGs were involved in the cell cycle. Flow cytometric analysis demonstrated that treatment of *P. cocos* induces cell cycle arrest at the G1 phase. Previous studies have shown that some anti-cancer drugs can inhibit cancer cells by arresting cell cycle progression and inducing apoptosis (Capozzi et al., 2012; Yuan et al., 2014). Notably, enriched KEGG analysis indicated that some DEGs are involved in pathways of nucleotide excision repair, mismatch repair, and DNA replication. It is well known that DNA damage is the triggering event of cell apoptosis (Roos et al., 2013). Consistently, the apoptosis effect of *P. cocos* was further confirmed by Hoechest 33342 and TUNEL staining assays. These results suggested that *P. cocos* causes DNA damage leading to cell cycle arrest and apoptosis.

It has been reported that promoting cell differentiation can be used as a therapeutic strategy for neuroblastoma treatment (Yang et al., 2019; Belluardo et al., 2021). Previous studies have also shown that the crude polysaccharides from *P. cocos* stimulated adipocyte differentiation of 3T3-L1 cells (Xun et al., 2011). Meanwhile, Neuro-2a cell lines were used as an *in vitro* neural differentiation cell model (Tremblay et al; 2010). Therefore, we have examined the biological effect of *P. cocos* on Neuro-2a cell differentiation. The present work shows that *P. cocos* induces differentiation of Neuro-2a cells, as evidenced by the development of neurite outgrowth.

Conclusion

P. cocos inhibits cell proliferation and induces Neuro-2a cell differentiation by mediating G1 cell cycle arrest and apoptosis.
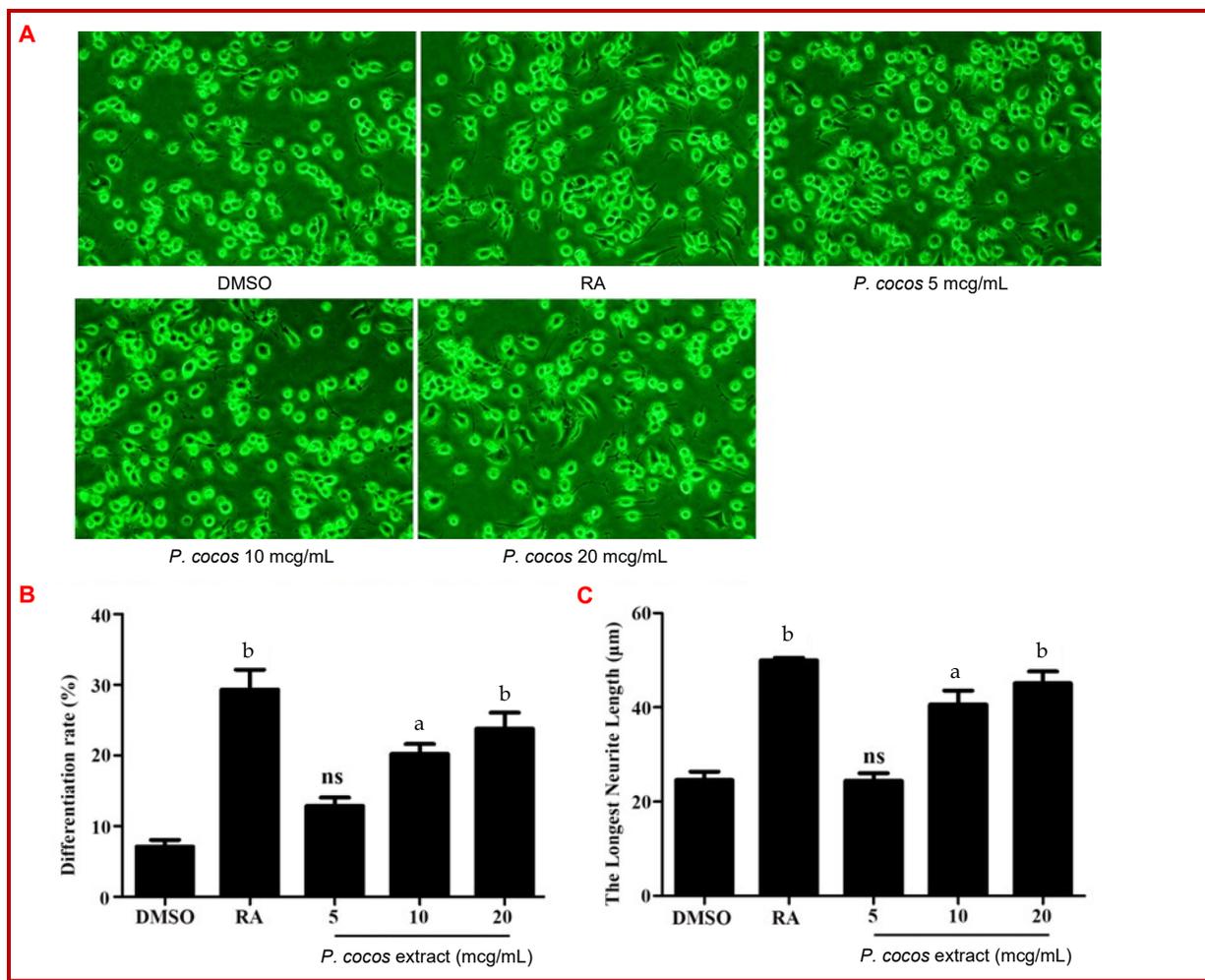
Figure 4: *P. cocos* promotes differentiation of Neuro-2a cells. Cell morphology is shown after Neuro-2a cells were treated with RA, various concentration (5-10 µg/mL) of *P. cocos* for two days (A). The changes in the differentiation rate (B) and the longest neurites length (C) in Neuro-2a cells treated with various concentrations (5-10 µM) of *P. cocos*. [a]$p<0.01$, [b]$p<0.001$, NS, not statistically significant. Student's t-test. At least 300 cells/group were analyzed in each experiment, n=3. Error bars, SEM

Financial Support

Conflict of Interest

Authors declare no conflict of interest

References

Belluardo N, Mudò G, Liberto VD, Frinchi M, Giuliani P. Investigating the role of guanosine on human neuroblastoma cell differentiation and the underlying molecular mechanisms. Front Pharmacol. 2021; 12: 658806.

Berthold F, Hero B. Neuroblastoma. Drugs.2000; 59: 1261-77.

Brodeur, Garrett M. Neuroblastoma: Biological insights into a clinical enigma. Nat Rev Cancer. 2003; 3: 203-16.

Canavate JLR. Poria cocos, a fungus with anti-inflammatory and immunoestimulant properties. Revista de Fitoterapia. 2010; 10: 147-56.

Capozzi A, Mantuano E, Matarrese P, Saccomanni G, Manera C, Mattei V, Gambardella L, Malorni W, Sorice M, Misasi R. A new 4-phenyl-1,8-naphthyridine derivative affects carcinoma cell proliferation by impairing cell cycle progression and inducing apoptosis. Anti-cancer Agent Me. 2012; 12: 653-62.

Cheng S, Gui Y, Shen S, Huang W. The antioxidant activity of triterpenes in the peels of *Poria cocos*. Med Plant. 2013; 8: 38-44.

Chang HH, Sheu F. A novel fungal immunomodulatory

protein (PCP) isolated from *Poria cocos* activates mouse peritoneal macrophage involved in toll-like receptor 4. FASEB J. 1991; 21: 702-15.

Dickey A, Schleicher S, Leahy K, Hu R, Hallahan D, Thotala DK. GSK-3b inhibition promotes cell death, apoptosis, and *in vivo* tumor growth delay in neuroblastoma Neuro-2A cell line. J Neurooncol. 2011; 104: 145-53.

Dong K, Wang G, Wang ZL, Wang X. Efficacy and safety of regorafenib versus dinutuximab with chemotherapy in Chinese children with neuroblastoma. Bangladesh J Pharmacol. 2019; 14: 32-35.

Eslami A, Lujan J. Western blotting: Sample preparation to detection. JoVE. 2010; 44: e2359.

Eun-Seok P, Chul K J, Chang JY, Seok PJ, Yi JS, Dae-Eun K, Bokyung K, Hwa-Sup S. Cardioprotective effects of rhamnetin in H9c2 cardiomyoblast cells under H_2O_2-induced apoptosis. J Ethnopharmacol. 2016; 153: 552-60.

Gordaliza M. Natural products as leads to anticancer drugs. Clin Transl Oncol. 2007; 9: 767-76.

Jeong JW, Lee H, Han M, Kim GY, Hong S, Park C, Choi Y. Ethanol extract of *Poria cocos* reduces the production of inflammatory mediators by suppressing the NF-kappaB signaling pathway in lipopolysaccharide-stimulated RAW 264.7 macrophages. BMC Complement Altern Med. 2014; 14: 101-08.

Jiang X, Tang GY, Yang J, Ding JC, Lin HW, Xiang XL. Synthesis of some new acylhydrazone compounds containing the 1,2,4-triazole structure and their neuritogenic activities in Neuro-2a cells. RSC Adv. 2020; 10: 18927-35.

Kumar A, Fan D, Dipette DJ, Singh US. Sparstolonin B, a novel plant derived compound, arrests cell cycle and induces apoptosis in N-myc amplified and N-myc nonamplified neuroblastoma cells. PLoS One. 2014; 9:e96343.

Lee JH, Lee YJ, Shin JK, Nam JW, Nah SY, Kim SH, Jeong JH, Kim YS, Shin M, Hong M. Effects of triterpenoids from *Poria cocos* Wolf on the serotonin type 3A receptor-mediated ion current in Xenopus oocytes. Eur J Pharmacol. 2009; 615: 27-32.

Lim HS, Jang Y, Moon BC, Park G. NF-κB signaling contributes to the inhibitory effects of *Bombyx batryticatus* on neuroinflammation caused by MPTP toxicity. Bangladesh J Pharmacol. 2021; 16: 96-102.

Mallepalli S, Gupta MK, Vadde R. Neuroblastoma: An updated review on biology and treatment. Curr Drug Metab. 2019; 20: 1014-22.

Maris JM, Hogarty M, Bagatell R, Cohn SL. Neuroblastoma. Lancet 2007; 369: 2106-20.

Pfy A, Tao HA, Dong WB, Zwz B, Glx B, Zfc B. Phytochemical and chemotaxonomic study of *Poria cocos* (Schw.) Wolf. Biochem Syst Ecol. 2019; 83: 54-56.

Roos WP, Kaina B. DNA damage-induced cell death: From specific DNA lesions to the DNA damage response and apoptosis. Cancer Lett. 2013; 332: 237-48.

Shang Y, Guo XX, Li WW, Rao W, Chen ML, Mu LN, Li SJ. Cucurbitacin-B inhibits neuroblastoma cell proliferation through up-regulation of PTEN. Eur Rev Med Pharmacol Sci. 2014; 18: 3297-303.

Shen S, Hou Y, Wu Y. Tongxinluo preserves the renal function in diabetic kidney disease via protecting the HK-2 cells from the patterns of programmed cell death. Bangladesh J Pharmacol. 2021; 16: 52-64.

Tang J, Nie J, Li DP, Zhu WJ, Zhang SP, Ma F, Sun Q, Song J, Zheng YL, Chen P. Characterization and antioxidant activities of degraded polysaccharides from *Poria cocos* sclerotium. Carbohyd Polym. 2014; 105: 121-26.

Towbin H, Staehelin T, Gordon J. Electrophoretic transfer of proteins from polyacrylamide gels to nitrocellulose sheets: Procedure and some applications. PNAS. 1979; 76: 4350-54.

Tremblay RG, Sikorska M, Sandhu J, Lanthier P, Ribecco-Lutkiewicz M, Bani-Yaghoub M. Differentiation of mouse Neuro 2A cells into dopamine neurons. J Neurosci Methods. 2010, 186: 60-67.

Xiang XL, Li SN, Zhang XJ, Shi L. Arhgef1 negatively regulates neurite outgrowth through activation of RhoA signaling pathways. FEBS Lett. 2016; 590: 2940-55.

Xun W, Liu H, Ling Z, Han D, Ning C, Li X, Cui H. Effects of the crude polysaccharides from *Poria cocos* on the proliferation and differentiation of 3T3-L1 cells. Res J Biol Sci. 2011; 6: 597-601.

Yang MS, Xu XJ, Zhang B, Niu F, Liu BY. Comparative transcriptomic analysis of rat versus mouse cerebral cortex after traumatic brain injury. Neural Regen Res. 2021; 16: 1235-43.

Yuan X, Li T, Xiao E, Zhao H, Li Y, Fu S, Gan L, Wang Z, Zheng Q, Wang Z. Licochalcone B inhibits growth of bladder cancer cells by arresting cell cycle progression and inducing apoptosis. Food Chem Toxicol. 2014; 65: 242-51.

Yang LQ, Zha YH, Ding J, Ye BW, Liu ML, Yan CH, Dong Z, Cui HJ, Ding HF. Histone demethylase KDM6B has an anti-tumorigenic function in neuroblastoma by promoting differentiation. Oncogenesis 2019; 8: 3-15.

Zhang M, Chiu L, Cheung P, Ooi V. Growth-inhibitory effects of a beta-glucan from the mycelium of *Poria cocos* on human breast carcinoma MCF-7 cells: Cell-cycle arrest and apoptosis induction. Oncol Rep. 2006; 15: 637-43.

Author Info
Xiaoliang Xiang (Principal contact)
e-mail: xiangxiaoliang225@163.com
First two authors contributed equally